

# Reciprocity and spectral effects of the degradation of poly(ethylene-terephthalate) under accelerated weathering exposures

Abdulkerim Gok <sup>1</sup>, Devin A. Gordon,<sup>2</sup> David M. Burns,<sup>3</sup> Sean P. Fowler,<sup>4</sup> Roger H. French <sup>2</sup>, Laura S. Bruckman <sup>2</sup>

<sup>1</sup>Department of Materials Science and Engineering, Gebze Technical University, Gebze, Kocaeli 41400, Turkey

<sup>2</sup>Department of Materials Science and Engineering, Solar Durability and Lifetime Extension (SDLE) Research Center, Case Western Reserve University, Cleveland, Ohio 44106

<sup>3</sup>3M Corporate Research Analytical Laboratory, 3M Center, Building 235-B-B-44, St. Paul, Minnesota 55144

<sup>4</sup>Q-Lab Corporation, 800 Canterbury Road, Westlake, Ohio 44145

Correspondence to: L. S. Bruckman (E-mail: laura.bruckman@case.edu)

**ABSTRACT:** Exposures of poly(ethylene-terephthalate) (PET) films were performed under xenon-arc (full spectrum) and fluorescent UVA-340 (UV only) irradiation to investigate the reciprocity principle and wavelength dependence of photodegradation in weathering. When the intensity of full spectral irradiance is increased from 5× to 50×, the reciprocity principle is not obeyed in this material system. The change in optical properties for PET is attributed to the corresponding longer exposure time of the 5× exposure that allows oxidative reactions to occur at lower irradiance. Full spectrum xenon-arc and fluorescent UVA-340 lamps have different spectral distributions and samples exhibit different material degradation mechanisms under each source. The UVA-340 exposure leads to more pronounced degradation relative to the full spectrum xenon-arc. This study shows that intensification of a single stressor in lab-based weathering experiments to accelerate degradation and the use of differing light sources are not sufficient to allow reliable determination of service lifetime of polymeric materials. © 2019 Wiley Periodicals, Inc. *J. Appl. Polym. Sci.* **2019**, 136, 47589.

**KEYWORDS:** degradation; optical properties; polyesters

Received 25 October 2018; accepted 19 January 2019

DOI: 10.1002/app.47589

## INTRODUCTION

Reciprocity is often taken as a base assumption used in the extrapolation of artificial accelerated weathering results to predict the service life of a material in real-world conditions. The law of reciprocity in photochemistry first proposed by Bunsen and Roscoe<sup>1</sup> states that the amount of photochemical effect induced by an exposure is directly proportional to the total radiant dosage, that is, irradiance ( $I$ ) × time ( $t$ ), regardless of the exposure duration required to deliver that dosage. Doubling the irradiance would therefore half the exposure time required and increasing it 10-fold would produce the same results in one-tenth the time as demonstrated by eq. (1).

$$I \times t = \text{constant} \quad (1)$$

The model of Schwarzschild<sup>2</sup> was later found to provide a better fit for the observed nonlinear response as shown in eq. (2). The more general relationship for polymer degradation takes the form of  $I^p$

where Schwarzschild's  $p$ -coefficient, usually ranges from 0.5 to 1, accounts for deviations from the linear reciprocity principle.<sup>3</sup>

$$I^p \times t = \text{constant} \quad (2)$$

A critical review of the reciprocity principle by Martin *et al.*<sup>4</sup> provides in depth discussion of the topic along with an extensive literature survey for a variety of materials; however, little has been published on polymers. In a study by Scott *et al.*,<sup>5</sup> yellowing of polystyrene and polycarbonate polymers showed noticeable deviations from reciprocity when exposed under xenon-arc full spectrum exposures with varying light intensities from 0.4 to 1.2 W m<sup>-2</sup> at 340 nm. Jorgensen *et al.*<sup>6</sup> tested polyvinyl-chloride and polycarbonate polymers over a broad range of total UV light irradiances and found that only polycarbonate showed linear reciprocity. The different reciprocity behavior of polycarbonate in these two studies may be attributed to the use of different light sources and specific polymer formulations. Similarly, Chin *et al.*<sup>7</sup>

performed degradation studies of unstabilized acrylic-melamine coatings under varying total UV light irradiances from 36 to 322 W m<sup>-2</sup>. Using various responses obtained through UV-visible spectroscopy and infrared absorption spectroscopy techniques, they found that photodegradation of the coatings exhibited very good reciprocity. However, Kollmann and Wood<sup>8</sup> showed that the rate of photo-oxidation of polypropylene was proportional to the light intensity. The deviation from linear behavior depended on the light source and the polymer formulation. White *et al.*<sup>9</sup> reported the failure of the reciprocity principle for PET degradation for comparable applied photo-doses under full spectrum light exposures. The specific degradation mechanisms differed depending on the irradiance level. At lower irradiance levels, the degradation path favored the oxidative route because of readily available oxygen; however, higher irradiance levels led to less oxidized product due to high photon flux and oxygen depletion. Pickett *et al.*<sup>10</sup> investigated yellowing of various polymeric materials under full spectrum light exposures up to 0.75 W m<sup>-2</sup> at 340 nm. While styrene/acrylonitrile and acrylonitrile/butadiene/styrene copolymers showed significant deviations from linear reciprocity, polycarbonate, polybutylene-terephthalate, polycarbonate/polybutylene-terephthalate, and polycarbonate/(acrylonitrile/butadiene/styrene) copolymers obeyed reciprocity with almost perfect linearity for yellowing over the applied irradiance range.

The use of an accelerated weathering test,<sup>11</sup> in combination with a simple acceleration factor<sup>12</sup> to calculate a service life is very appealing, but it should not be confused with service life prediction.<sup>13,14</sup> Such a calculation is not based on a fundamental understanding of materials properties, the stresses imposed by the exposure conditions, or the degradation mechanisms and pathways involved along with their dependence on irradiance, temperature, or relative humidity. The service life of a material is the length of time a material in an end-use application will maintain a level of properties adequate to fulfill its intended function. Failure occurs when one or more of the material properties, such as appearance, physical, or mechanical properties, fall below the level required by the application.<sup>15</sup> Service life prediction requires an extensive body of experimental data and multivariate statistical modeling involving both lab-based accelerated and real-world weathering exposures and their cross-correlation.<sup>16</sup> The use of standardized tests with their typical pass/fail criteria do not incorporate the experimental requirements to account for the complexity of in-use conditions needed for accurate prediction. While standardized industry tests are admittedly useful for detecting manufacturing flaws in short time frames and for supply chain and quality validation, they do not provide insights into degradation mechanisms, rates, and pathways.<sup>17</sup> In actual use conditions, additional challenges emerge due to uncontrolled factors such as spectral effects, nonuniform conditions of irradiance, temperature, and moisture, thermal cycling, or mechanical stresses that affect material properties by inducing physical and chemical changes. Accounting for these factors further complicates the task of cross-correlation. Cross-correlation of various exposure conditions, such as lab-based exposures and real-world weathering stressors that can be initially represented by Köppen-Geiger climatic zones,<sup>18,19</sup> is vital for accurate service life prediction.

A basic precept of artificial weathering is that in order to reliably reproduce the effects of natural sunlight, one must use a light source that closely matches the spectral distribution of natural sunlight. Artificial sources that include radiation shorter than the solar cut-on at 290 nm will typically induce degradation faster, but this very high energy radiation has also been found to alter the degradation pathway of a material and become non-predictive of real-world exposures.<sup>20</sup> Fluorescent UVA-340 lamps and xenon-arc lamps with second generation daylight filters provide the best technical simulation of natural sunlight available today. UVA-340 lamps are a good match to sunlight up to 360 nm, after which the lamp irradiance drops off sharply. Xenon-arc lamps are broad band sources that emit from the ultraviolet all the way up through the infrared, just like natural sunlight, and with second generation daylight filters, provide a near exact match to sunlight from the solar cut-on at 295 nm.<sup>21</sup> Over the course of time a wide variety of artificial sources have been used for conducting artificial weathering of photovoltaic materials, components, and systems. While some produce highly accelerated degradation, the degradation produced has not always been predictive of long-term natural weathering. The International Electrotechnical Commission (IEC-TS82 WG2) has been developing a standard technical specification for conducting accelerated weathering tests to qualify polymeric materials and components for photovoltaic modules.<sup>22,23</sup> Based on years of collaborative research by governments, academics, and industry, the IEC has recommended UVA-340 and xenon-arc lamps with second generation daylight filters, and only these sources, for durability testing of module materials.

Caution, however, must be taken when using and comparing the responses obtained under these different light sources in lab-based artificial exposures. A material's action spectrum, the wavelength dependent degradation response,<sup>15</sup> is very important for understanding spectral effects of different light sources because materials differ in their sensitivity to specific regions of the spectrum.<sup>24</sup> Where action spectra are not available the alternative is to use a full spectrum source that closely matches natural sunlight for cross-correlation studies. Full spectrum filtered xenon-arc sources provide the best match to natural sunlight and are most commonly used for polymer degradation. Fluorescent UVA-340 lamp exposures replicate the short-wavelength, high energy solar ultraviolet that is usually the most damaging part of the solar spectrum and are used primarily to screen for rapid degradation. Theoretically one could use sources that do not match the spectral distribution of sunlight given the source provides sufficient energy within the material's action spectrum to induce degradation along the same pathways and to the same end state as sunlight. Characterizing a material's action spectrum requires specialized instrumentation and technical knowledge and is rarely done.<sup>25,26</sup> The effect of temperature during accelerated testing is another critical factor in polymer degradation. Depending on the photo-dose applied and the optical absorption of the material being tested, even common chamber temperatures or black panel temperatures may produce different degradation pathways in a particular polymer type due to thermal effects. Wypych *et al.*<sup>27</sup> reported that degradation of acrylic sealants under UVA-340 exposure was faster than under full spectrum exposure

at comparable photo-doses and attributed this to differences in the specimen temperatures under each exposure condition. While the spectral irradiance of fluorescent UVA-340 lamps is limited to the ultraviolet, full spectrum sources provide irradiance over a much broader range of wavelengths from the UV into the infrared. However, radiant heating by the light source is often unaccounted for in artificial weathering, especially at high irradiance levels.

PET is a key material in many industrial applications used outdoors, specifically for photovoltaic module backsheets. Photodegradation of PET involves a multistep degradation pathway involving photolysis producing backbone chain scission and subsequent photo-oxidation, given enough oxygen and time to enable these mechanisms. Degradation of the polymer backbone through chain scission produces fluorescent mono-hydroxyterephthalate units giving rise to the optical absorption at 340 nm and the corresponding fluorescence emission at 460 nm. These hydroxylated phenolic groups then undergo oxidation reactions, forming quinones, leading to strong optical absorbance due to their high extinction coefficients associated with the absorption of visible light and thus yellowing extending into the visible region.<sup>28–31</sup> However, haze formation is generally caused by light scattering due to impurities, inhomogeneities, or crystallites within the bulk, or due to increased roughness, abrasion, and cracking (or crazing) on the surface. It is a stochastic process, that is, spatially localized formation of light scattering moieties, and so it does not uniformly form across the sample volume as seen with yellowing. It is mostly induced by hydrolytic degradation under heat and humidity, and light only has little or no effect on its formation.<sup>31</sup>

In this paper, photodegradation experiments of unstabilized PET films were performed under fluorescent UVA-340 and full spectrum xenon-arc light sources at a range of irradiance levels to determine the impact of reciprocity across irradiance levels and investigate wavelength dependent spectral effects on the degradation pathways. Considering the activation of multiple and competing degradation mechanisms under real-world exposures that involve multiple combined stressors and varying stress levels, this study suggests that accelerating the degradation by escalating a single stressor in lab-based experiments and the use of different light sources are not a reliable approach for service lifetime prediction.

## EXPERIMENTAL

### Materials

In this degradation science study, the epidemiological data science approach<sup>33</sup> was applied in a laboratory-based, randomized, longitudinal study design.<sup>34,35</sup> Samples of unstabilized PET films (Dupont-Teijin Melinex 454, 75  $\mu\text{m}$ ) were randomly assigned to exposure conditions and followed over time with repeated measurements. The measurements were conducted after the samples had reached room temperature. The results were plotted for all samples (including replicates) as individuals.

### Exposures

Full spectrum light exposures were performed using two different solar simulators. The 5 $\times$  exposure used a Newport diverging beam solar simulator (Model 92190) with a 1.6 kW xenon-arc lamp and a concentrator lens unit (Model SP81030-DIV). The

5 $\times$  exposure had a full spectrum irradiance of  $\sim 5 \text{ kW m}^{-2}$  with an air mass (AM) 1.5G filter (Model 81388) to spectrally match the solar irradiance according to the ASTM G173-03 standard.<sup>36</sup> A Spectrolab solar simulator (Model XT-30) with a 3 kW xenon-arc lamp and an AM 1.5G filter was used to produce a full spectrum irradiance of  $\sim 50 \text{ kW m}^{-2}$  for the 50 $\times$  exposure. It uses a reflective homogenizer unit consisting of four-sided concentrating mirror and a water cooled ultrahigh purity silica lens assembly. The irradiance under each simulator was determined by a Newport (Model 1918-R) and a Thorlab (Model PM100D) thermopile power sensors located under the sample stage to quantify the irradiance and its stability over the exposure time. The sample temperature under both exposure conditions were measured around 35  $^{\circ}\text{C}$  with a FLIR (Model T300-IR) infrared camera.

For the UV light exposure, a Q-Lab QUV weathering tester (Model QUV/Spray with Solar Eye Irradiance Control) was used with UVA-340 fluorescent lamps producing UV spectral power distribution that closely matches the AM 1.5 spectrum between 280 and 360 nm. The UVA-340 irradiance set-point was  $1.55 \text{ W m}^{-2}$  at 340 nm. The chamber black panel temperature is held at 70  $^{\circ}\text{C}$  corresponding to a modified ASTM G154 Cycle 4 standard<sup>25</sup> without the condensing humidity cycle. Comparison of the ASTM G173-03 standard (AM 1.5), full spectrum xenon-arc, and fluorescent UVA-340 light sources can be seen in Figure 1.

For more accurate comparison between the two light sources, we used the photo-dose calculated between 280 and 360 nm ( $\text{UVA}_{<360}$ ) as shown in eq. (3) where  $\text{UVA}_{<360}$  is the radiant exposure (photo-dose) between 280 and 360 nm ( $\text{J m}^{-2}$ ),  $E_{\lambda}$  is the irradiance ( $\text{W m}^{-2}$ ),  $\lambda$  is the wavelength, and  $t$  is the exposure time.<sup>37</sup>

$$\text{UVA}_{<360} = \int_0^t \int_{280}^{360} E_{\lambda} d\lambda dt \quad (3)$$

Because the spectral irradiance of the fluorescent UVA-340 lamp drops off sharply after 360 nm, the correlations of different exposures on the total UV (TUV) photo-dose basis would be poor. For instance, 1  $\text{MJ m}^{-2}$  TUV dose from a fluorescent UVA-340 lamp is much more damaging than that from a xenon-arc lamp, since for the same number of photons, the UVA-340 lamp's photons are at higher photon energies. The full spectrum xenon-arc lamps used in this study goes only up to 1700 nm as even though its integrated irradiance over the entire range is almost identical to AM 1.5 standard. However, the xenon-arc has smaller fraction of  $\text{UVA}_{<360}$  irradiance compared to that of the AM 1.5 spectrum. Numerically,  $\text{UVA}_{<360}$  region corresponds to 1.93% of the AM 1.5, but 0.55% of the xenon-arc source in terms of integrated  $\text{UVA}_{<360}$  irradiance. Therefore, for the same amount of exposure time, AM 1.5 has a greater  $\text{UVA}_{<360}$  photo-dose content.

### Study Protocol

Spectral characteristics of 5 $\times$  and 50 $\times$  full spectrum and fluorescent UVA-340 irradiance exposures are given in Table I. Four samples were exposed to 5 $\times$  and 50 $\times$  concentrated full spectrum light for a total  $\text{UVA}_{<360}$  photo-dose of  $\sim 110 \text{ MJ m}^{-2}$ . The total exposure time for the 5 $\times$  exposure was 1110 h and the samples were measured at the following exposure steps: 0 h (0  $\text{MJ m}^{-2}$ ), 158.6 h (15.58  $\text{MJ m}^{-2}$ ), 317.2 h

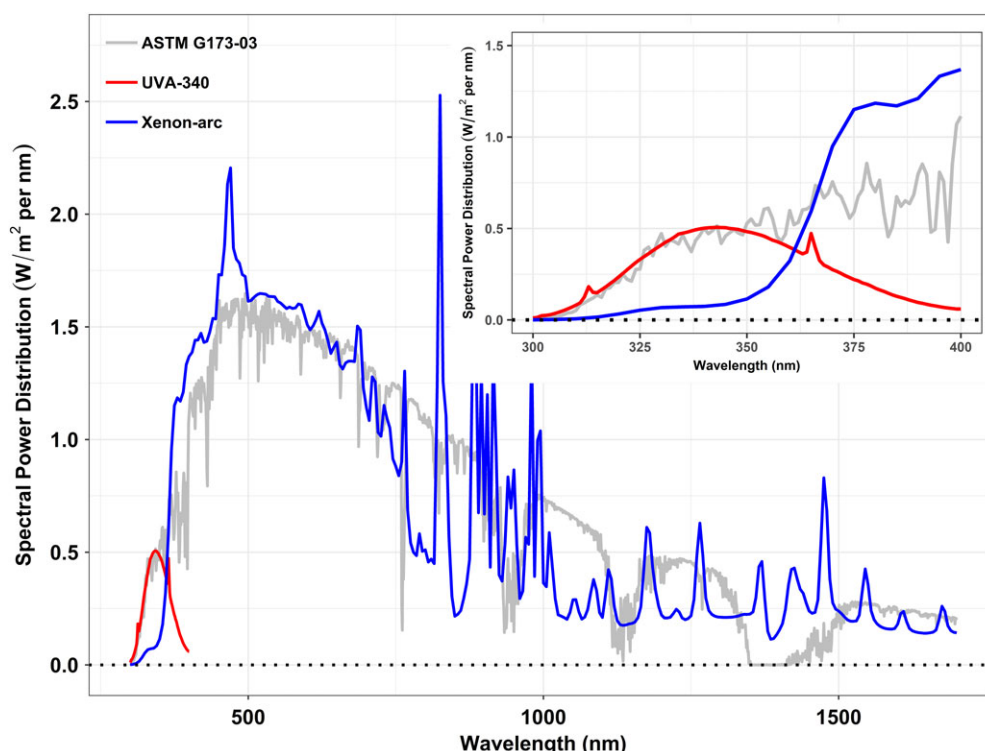


**Figure 1.** Spectral power distributions of the ASTM G173-03 standard (AM 1.5), xenon-arc full spectrum, and fluorescent UVA-340 light sources. The inset shows the UV region between 300 and 400 nm. [Color figure can be viewed at [wileyonlinelibrary.com](http://wileyonlinelibrary.com)]

(31.2 MJ m<sup>-2</sup>), 475.8 h (46.8 MJ m<sup>-2</sup>), 792.9 h (77.9 MJ m<sup>-2</sup>), and 1110 h (109.1 MJ m<sup>-2</sup>). The total exposure time for the 50× exposure was 111 h and the samples were measured at the following exposure steps: 0 h (0 MJ m<sup>-2</sup>), 15.9 h (15.58 MJ m<sup>-2</sup>), 31.7 h

(31.2 MJ m<sup>-2</sup>), 63.4 h (62.3 MJ m<sup>-2</sup>), and 111 h (109.1 MJ m<sup>-2</sup>). For the spectral effects study, 15 samples of PET were exposed under UVA-340 light to a total UVA<sub><360</sub> photo-dose of ~110 MJ m<sup>-2</sup>. The total UVA-340 exposure time was 504 h and samples were measured at the following exposure steps: 0 h (0 MJ m<sup>-2</sup>), 168 h (36.7 MJ m<sup>-2</sup>), 336 h (73.4 MJ m<sup>-2</sup>), and 504 h (110 MJ m<sup>-2</sup>).

**Table I.** Spectral Characteristics of 5× and 50× Full Spectrum and Fluorescent UVA-340 Irradiance Exposures Giving the Total Amount of Photo-Dose and Time for Each Exposure Type

	Spectral region <sup>a</sup>	5×	50×	UVA-340
Irradiance (W m <sup>-2</sup> )	Full spectrum	5000	5000	84.54
	TUV	265.21	2652.12	85.54
	UVA <sub>&lt;360</sub>	27.30	273.00	60.65
Exposure time (h)		1110	111	504
Photo-dose (MJ m <sup>-2</sup> )	Full spectrum	19 980	19 980	153.40
	TUV	1059.80	1059.80	153.40
	UVA <sub>&lt;360</sub>	109.10	109.10	110.05

<sup>a</sup> Each spectral region represents a portion of total solar radiation. Full spectrum refers to all irradiance from 280 to 4000 nm, TUV spectrum refers to total UV irradiance from 280 to 400 nm, and UVA < 360 spectrum refers to irradiance from 280 to 360 nm. The region between 280 and 360 nm was chosen for the UVA < 360 spectrum because the spectral curve of the UVA-340 fluorescent light source has a close match to AM 1.5 sunlight in this region. Critically, the cut-on wavelength, the shortest wavelength at which significant irradiance can be measured, is approximately equivalent for each light source and the AM 1.5 spectrum.

## Evaluations

A HunterLab UltrascanPro colorimeter was used to measure yellowness index (YI) and haze (%) values of the exposed samples. YI is a measure that quantifies the change in color of a sample toward yellow as defined by the ASTM E313 standard<sup>38</sup> using the D65 standard illuminant with 10° viewing angle (D65/10°) in transmission mode calculated using eq. (4) where  $X_{CIE}$  (red),  $Y_{CIE}$  (green), and  $Z_{CIE}$  (blue) represent CIE tristimulus values. Haze (%) is calculated as the percentage of incident light in the spectral range between 380 and 780 nm that is scattered by more than 2.5° as defined by the ASTM D1003-13 standard.<sup>39</sup> It is the ratio of diffuse transmission to total transmission as shown in eq. (5).

$$YI = \frac{100(1.3013X_{CIE} - 1.1498Z_{CIE})}{Y_{CIE}} \quad (4)$$

$$Haze(\%) = 100 \times \frac{T_{diffuse}}{T_{total}} \quad (5)$$

For the optical absorbance changes in the exposed samples, an Agilent Cary 6000i UV-Vis-NIR spectrometer with a DRA-1800 diffuse reflectance accessory was used. The center mount



absorbance spectra were taken from 250 to 900 nm every 0.50 nm with a scan rate of 112.5 nm min<sup>-1</sup> and a spectral bandwidth of 4.00 nm. Spectra were first corrected for zero absorbance between 600 and 800 nm and then normalized for the sample thickness to get the Abs cm<sup>-1</sup> (base 10) metric.

An Agilent Cary Eclipse Fluorescence spectrophotometer was used to take fluorescence spectra of the exposed samples. The emission spectra were collected between 300 and 800 nm every 1 nm with a scan rate of 120 nm min<sup>-1</sup> with excitation at 340 nm. Excitation and emission slits were set to 5 nm with photomultiplier tube voltage of 650 V.

Along with YI and haze (%), spectral data points were extracted from UV-Vis and fluorescence spectra and plotted against UVA<sub><360</sub> photo-dose for ease of comparison for both reciprocity and spectral effects studies at the following wavelengths: Optical absorbance at 312 nm for the fundamental absorption edge, optical absorbance at 340 and 400 nm for the formation of light absorbing chromophores, and fluorescence emission intensity at 460 nm with 340 nm excitation.

## RESULTS

Optical absorbance spectra of PET samples exposed to a total UVA<sub><360</sub> photo-dose of ~110 MJ m<sup>-2</sup> are given in Figure 2 showing PET's degradation under the two full spectrum and fluorescent UVA-340 light exposures. Even though the same UVA<sub><360</sub> photo-dose applied under the three exposure conditions, optical absorption characteristics vary tremendously. There is a severe increase in optical absorbance when exposed under the UVA-340 exposure and a moderate increase under the 5× full spectrum exposure, however, the spectrum of 50× is almost identical to the unexposed baseline spectrum throughout the entire region.

The evaluations for the reciprocity study are shown in Figure 3. While a small increase is seen in YI for the 5× exposure, bleaching under the 50× exposure is observed with a small decrease [Figure 3(a)]. Both exposures exhibit a similar trend in haze formation [Figure 3(b)] with a small increase over time; however, large variation in haze (%)

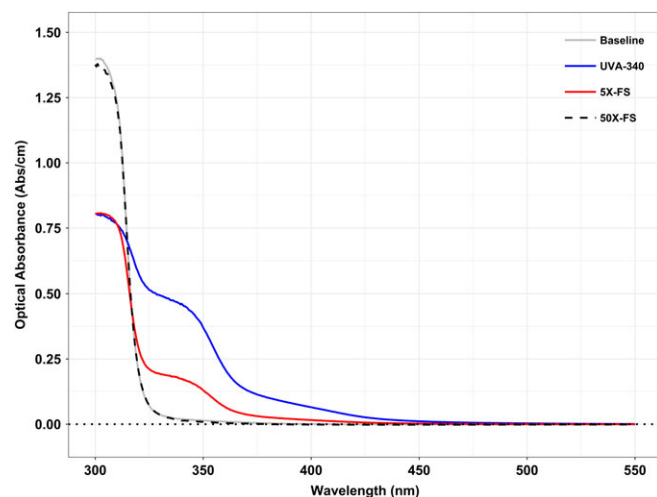


**Figure 2.** Optical absorbance spectra of PET exposed under the two xenon arc full spectrum and fluorescent UVA-340 light sources. [Color figure can be viewed at [wileyonlinelibrary.com](http://wileyonlinelibrary.com)]

data makes it difficult to compare the two exposures. For the 5× exposure, the absorbance at the fundamental absorption edge at 312 nm [Figure 3(c)] exhibits a decrease over successive dose steps indicating a chain scission process, but it remains about constant under the 50× exposure. This suggests that the longer exposure time of the 5× exposure has led to photo-oxidative reactions leading to polymer backbone degradation. The much shorter exposure time of the 50× exposure appears to have negligible impact on the polymers. The increased optical absorbances at 340 and 400 nm are evident for the 5× exposure [Figure 3(d,e)]; however, there is a slight decrease for the 50× exposure, particularly at 400 nm, likely due to the bleaching of excess monomer and surface coating on the film surface with high irradiance. This behavior is consistent with the diminished YI values under the 50× exposure. The fluorescence emission (ex. 340 nm) at 460 nm under the 5× exposure [Figure 3(f)] is due to the formation of hydroxylated species and in line with the optical absorbance at 340 nm as they refer to the same photochemical process.

The evaluations for the spectral effects study are shown in Figure 4. While a drastic increase (roughly from 0.5 to 3.5) in YI is evident under the UVA-340 exposure, full spectrum exposure only shows a slight increase (roughly from 0.25 to 0.75) for the equal amount of applied UVA<sub><360</sub> photo-dose [Figure 4(a)]. Similar to the reciprocity study, the haze formation exhibits noisy data [Figure 4(b)]. The fundamental absorption edge at 312 nm [Figure 4(c)] exhibits a decrease for the full spectrum exposure, but there appears to be no obvious trend under the UVA-340 exposure. There is a marked decrease at the first exposure step, but it slightly increases afterward. Under the UVA-340 exposure, the optical absorbance at 340 nm [Figure 4(d)] and 400 nm [Figure 4(e)] both show a dramatic increasing rate, ~10-fold, with a linear change point around the first exposure step. Even though the full spectrum exposure caused a noticeable increase in the optical absorbance at these wavelengths, the rate of change is much faster under the UVA-340 exposure, leading to approximately five times greater absorbance at the end of exposure cycle for the equal amount of UVA<sub><360</sub> photo-dose. This indicates that the UVA-340 exposure causes greater degradation than the full spectrum exposure. The fluorescence characteristics, however, exhibit opposite trends [Figure 4(f)]. The emission intensity (ex. 340 nm) at 460 nm increases with successive dose steps under the full spectrum exposure. Yet, it increases tremendously with the first exposure step and then drops under the UVA-340 exposure.

## DISCUSSION

### Degradation Mechanisms and Pathways of PET

The degradation rate of PET films, as measured by the change in optical absorbance shown in Figures 2 and 3, on an equivalent UVA<sub><360</sub> photo-dose basis, does not obey the principle of reciprocity when exposed to 5× and 50× full spectrum light. The correspondingly longer exposure times at 5× irradiance, as compared to 50× full spectrum irradiance, enables oxidative degradation mechanisms causing noticeable changes in the polymers' structure as seen in Figure 3(c). With the 50× full spectrum exposure (higher intensity for shorter time), decreased yellowing rates are observed in Figure 3(a) with little changes in the polymer backbone. At higher intensities, the formation of free radicals due to high degree

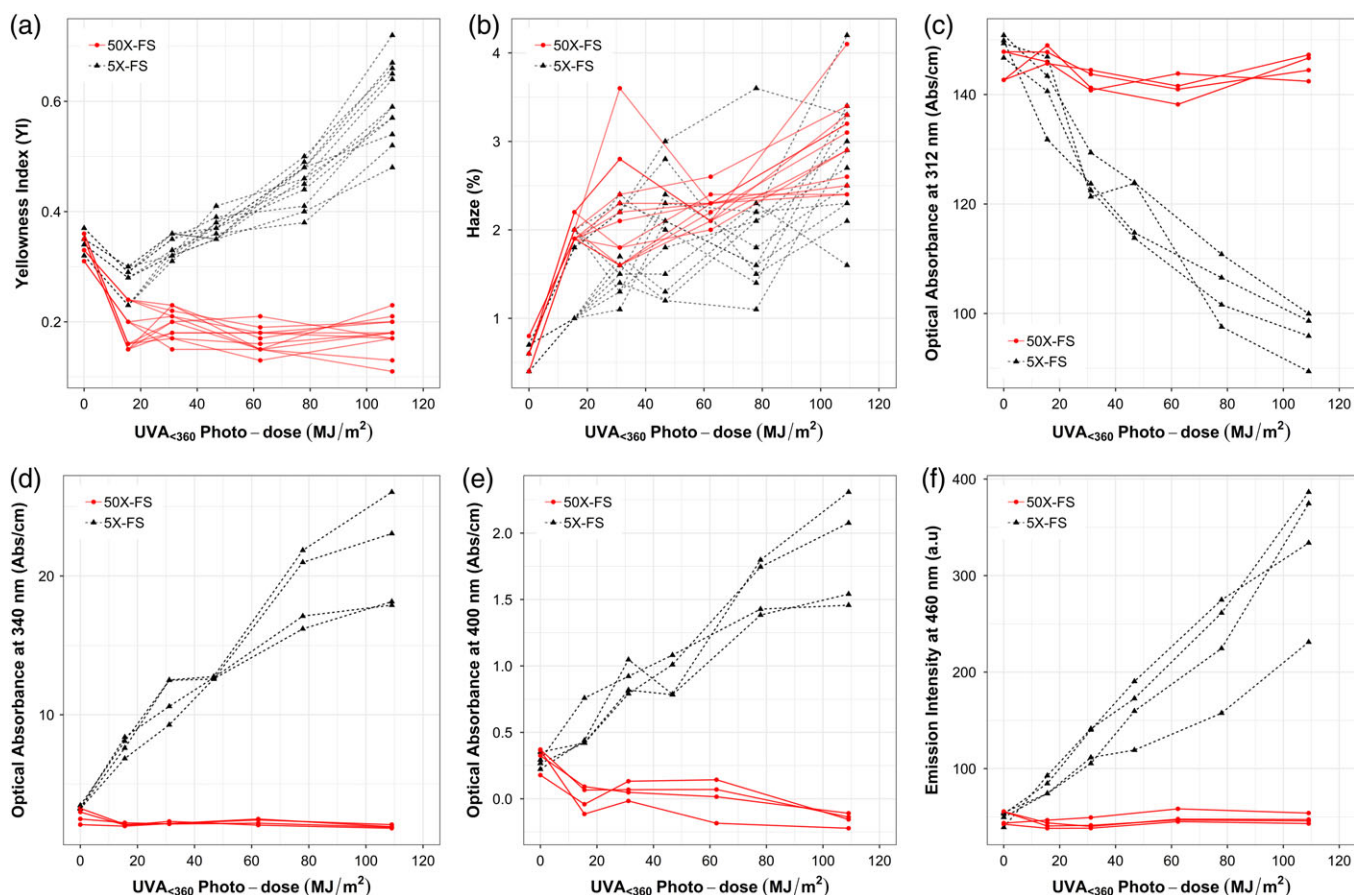


**Figure 3.** (a) Yellowness index (YI), (b) Haze (%), (c) optical absorbance at 312 nm for the fundamental absorption edge, (d) optical absorbance at 340 nm, (e) optical absorbance at 400 nm, and (f) fluorescence emission (ex. 340 nm) at 460 nm, under the 5× and 50× full spectrum xenon-arc light exposures. [Color figure can be viewed at [wileyonlinelibrary.com](http://wileyonlinelibrary.com)]

of photon flux and the rate of recombination of these free radicals is increased and the quantum yield of the overall degradation and the diffusion of oxygen and thus the rate of photo-oxidation reactions are diminished.<sup>15</sup> It appears that the photo-oxidative degradation path is favored under the low intensity light exposure as the availability and diffusion of oxygen have a strong impact on the degradation pathway. Competing mechanisms between the formation of fluorescing hydroxylated species and discoloring quinones may be present depending on the presence (or effectiveness) of oxygen in the reaction pathway. Moreover, since samples were taken out for measurement at certain time steps (every 24–48 h), these can be considered as dark cycles<sup>40</sup> and a possible recovery process could result in less degradation than expected under the 50× full spectrum exposure.

The spectral effects (full spectrum xenon-arc versus UVA-340 fluorescence) study illuminates additional aspects of PET's degradation mechanisms and pathways as shown in Figures 2 and 4. The UVA-340 exposure caused greater degradation, as evidenced by changes in the optical properties, compared to the full spectrum exposure on an equivalent UVA<sub>360</sub> photo-dose basis. Pickett<sup>10</sup> reported that a UVA-340 source causes greater yellowing than a xenon-arc source, as seen in Figure 4(a), due to the lack of visible light in the fluorescent exposure, which can photo-bleach the chromophores. The reduced fluorescence emission intensity

at 460 nm after the first exposure step shown in Figure 4(e) also suggests the oxidation process of hydroxylated units into quinonoid structures causing a strong increase in the yellowness of polymers. However, it is important in the current study to also consider the role of thermolysis and the associated thermal activation of other photodegradation mechanisms, since the UVA-340 exposure was performed at a higher temperature (at 70 °C) as specified by the standard and the 5× full spectrum exposure was performed at uncontrolled conditions (~35 °C). Photodegradation is often accelerated by increased temperature leading to secondary reactions between photodegradation by-products. Each 10 °C increase in temperature increases the degradation reaction rate by 33% even under constant irradiance.<sup>20</sup> The synergistic interactions make for a complex network of degradation pathways that are impacted by the specifics of the light, oxygen, and moisture, and their quantities (or levels), and the resulting rates of diffusion and reaction.

### Reciprocity Principle

Cross-correlation of accelerated degradation studies to real-world exposure conditions are often assessed based on the reciprocity principle, yet it only applies under very restrictive materials and exposure conditions.<sup>41</sup> Changing the light intensity, without changing the spectral characteristics of the light sources, changed

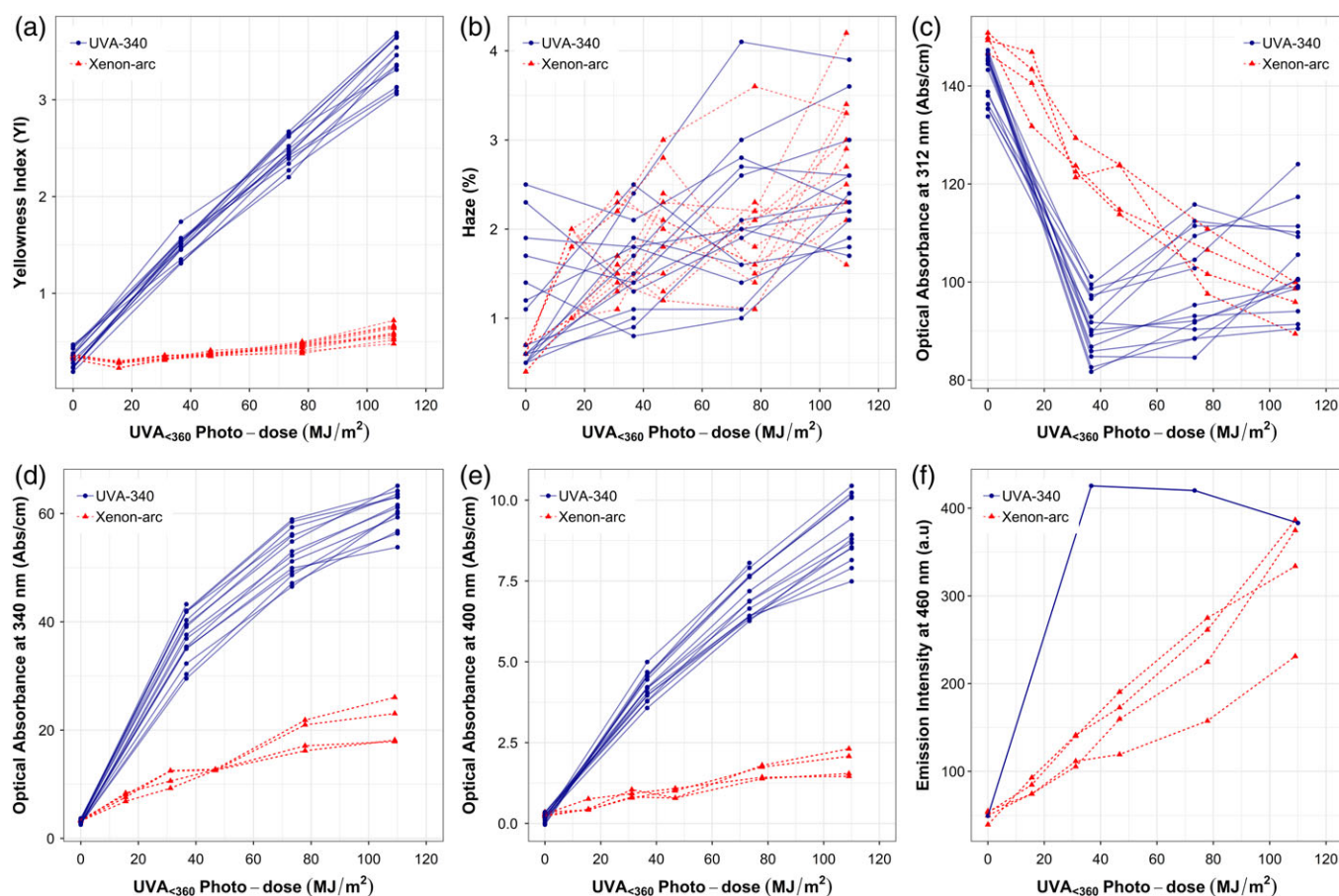


**Figure 4.** (a) Yellowness index (YI), (b) Haze (%), (c) optical absorbance at 312 nm for the fundamental absorption edge, (d) optical absorbance at 340 nm, (e) optical absorbance at 400 nm, and (f) fluorescence emission (ex. 340 nm) at 460 nm, under the xenon-arc full spectrum and fluorescent UVA-340 light exposures. [Color figure can be viewed at [wileyonlinelibrary.com](http://wileyonlinelibrary.com)]

the degradation responses noticeably for an equal amount of total UVA<sub><360</sub> photo-dose as shown in Figures 2 and 3. Considering the complex nature of stressors and stress levels in the real-world and their mutual effects on polymer degradation, the use of lab-based tests with a single stressor or multiple stressors with a constant stress level could not accurately predict lifetime. Furthermore, additional stressors in real-world such as light cycles during day and night, and temperature and relative humidity changes during the day, and throughout the year, can introduce physical or mechanical degradation such as crazing and cracking in polymeric materials. Depending on the climatic conditions, increased time of wetness due to dew formation can also increase the humidity content absorbed by materials more than that caused by rain or ambient relative humidity. Therefore, the rate of hydrolytic degradation may be different under accelerated exposures. Cloudiness and soiling can significantly alter the amount and spectral characteristics of the irradiance and impact the photodegradation rates. For good correlation, the type of light, the test, ambient, and sample temperatures, the humidity type and its concentration, and the exposure cycles should be taken into consideration.

Even when any form of reciprocity is obtained for a material, it should only be applied to the same material since any change in material chemistry can cause deviations from the previously defined

reciprocal behavior. For reciprocity to apply, there should be only one compound in the material that is affected by light, because different additives might react to light differently at varying light intensities, and lead to different degradation mechanisms and pathways. For instance, in case of an addition of UV stabilizer, the onset of degradation (i.e., induction period) will give rise to a change point: a region where the UV stabilizer hinders the photochemical reactions followed by an increased rate of degradation after the stabilizer is degraded. Depletion kinetics of the stabilizer content can also change under low and high intensity light and make the assumption of reciprocity nearly inapplicable. The degradation reaction should not saturate or self-propagate over time and there should be no accumulation of degradation by-products that can lead to subsequent degradation. So realistic irradiance levels should be applied, and the spectral characteristics of light and additional stressors and stress levels must be held constant in experiments to determine if the reciprocity principle is valid.

### Wavelength Sensitive Degradation

Xenon-arc light sources that closely match the entire solar spectrum and fluorescent UV light that closely match the UV portion of the solar spectrum are widely used to replicate the damaging effects of solar radiation. Changing the light source (i.e., changing the spectral characteristics of the lights applied) altered the



degradation responses significantly even for an equal amount of total UVA<sub><360</sub> photo-dose as shown in Figures 2 and 4. The effectiveness of the two exposure types depends on the activation spectrum and the intended use of the material, as degradation mechanisms can vary by the different regions of the solar spectrum and in-use environment. The short wavelength light can mostly be absorbed by the polymer surface and can cause degradation associated with surface properties like gloss loss, crazing, and yellowing as seen in Figure 4(a); however, the longer wavelength light can penetrate deeper into the bulk and cause changes associated with the physical integrity of polymers as seen in Figure 4(c). It is essential to perform a prior real-world study to determine the activation spectrum of the material of interest and determine if either approach closely mimics the degradation mechanisms active under natural weathering. If both chambers reproduce similar degradation to what is seen during real-world exposure, then the fluorescent UVA source can be the choice of exposure as it costs less than the full spectrum xenon-arc tester. Precise temperature and humidity control may be required for specific degradation mechanisms. For example, degradation in visual appearance (i.e., change in color or gloss) can be replicated under light exposures, but the presence of humidity can cause a loss in mechanical properties in real-world use. Even the same temperature is set in both testers, varying sample temperatures that lead to different degradation mechanisms can be observed depending on the materials (i.e., light or dark colored), temperature sensor type, and the way sensors are being cooled. These will give insights for weathering experiments on when a full spectrum exposure is needed and when a fluorescent UVA exposure can be used to reproduce degradation observed in real-world.

### Service Lifetime Prediction

Like this study, the reciprocity principle does not hold in many applications due to the specifics of material and exposure conditions even under well-controlled lab-based experiments. The total UVA<sub><360</sub> photo-dose of 110 MJ m<sup>-2</sup> applied in the spectral effects study corresponds ~to 274 days (0.75 years) of real-world exposure<sup>42</sup> in Phoenix, AZ (a BWh Köppen-Geiger climate zone). For an equal photo-dose content, increasing the intensity from 5× (for ~46 days of exposure) to 50× (for ~4.6 days of exposure) resulted in varying degradation mechanisms, as shown in Figure 3, making the idea of correlation to 0.75 years in real-world conditions impossible. The degradation rate under real-world exposure conditions could not be estimated just by accelerating one factor in lab-based exposures, disproving the assumption of having the same degradation mechanisms under high stress levels and actual service conditions.<sup>43</sup> The validity of service lifetime prediction based on lab-based accelerated weathering exposures depends on significant experimental effort and multivariate statistical modeling and requires real-world data to cross-correlate with accelerated exposures.

### CONCLUSIONS

Degradation of PET did not follow the linear reciprocity principle when the full spectrum irradiance level was increased from 5× to 50× for an equal UVA<sub><360</sub> photo-dose. The degradation mechanisms were found to differ depending on the intensity level. Longer

exposure times in the 5× full spectrum exposure allowed oxidative reactions to take place compared to the 50× exposure. The use of different light sources, even for an equal amount of total photo-dose, revealed wavelength dependent degradation. The UVA-340 exposure caused more pronounced changes in optical absorbance properties compared to the full spectrum exposure. Additional factors such as temperature were shown to play a role in accelerating the photo-oxidation reactions. Considering the deviation from reciprocity and introduction of new degradation pathways under varying light intensities and sources, the use of accelerated exposures carries serious risks for service lifetime prediction.

### ACKNOWLEDGMENTS

This research was performed at the Solar Durability and Lifetime Extension (SDLE) Research Center (funded through Ohio Third Frontier, Wright Project Program Award Tech 12-004) at Case Western Reserve University. The authors would like to acknowledge funding from 3M Corporate Research Laboratory (Agreement Control Number: 1401945) and support from Q-LAB and thank Tekra for providing samples.

### REFERENCES

1. Bunsen, R.; Roscoe, H. *Ann. Phys.* **1859**, 184, 193.
2. Schwarzschild, K. *Astrophys. J.* **1900**, 11, 89.
3. White, K. M.; Fischer, R. M.; Ketola, W. D. In *Service Life Prediction of Polymeric Materials*; Martin, J. W.; Ryntz, R. A.; Chin, J.; Dickie, R. A., Eds.; Springer: US, **2009**. p. 71.
4. Martin, J. W.; Chin, J. W.; Nguyen, T. *Prog. Org. Coat.* **2003**, 47, 292.
5. Scott, K. P.; Iii, H. K. H. In *Service Life Prediction of Polymeric Materials*; Martin, J. W.; Ryntz, R. A.; Chin, J.; Dickie, R. A., Eds.; Springer: US, **2009**. p. 83.
6. Jorgensen, G.; Bingham, C.; King, D.; Lewandowski, A.; Netter, J.; Terwilliger, K.; Adamsons, K. In *Service Life Prediction*; Martin, J. W.; Bauer, D. R., Eds.; Vol. 805, American Chemical Society: Washington, DC, **2001**. p. 100.
7. Chin, J.; Nguyen, T.; Byrd, E.; Martin, J. *JCT Res.* **2005**, 2, 499.
8. Kollmann, T. M.; Wood, D. G. M. *Polym. Eng. Sci.* **1980**, 20, 684.
9. White, K. M.; Koo, H.-J.; Kanuga, K.; Battiste, J. L. In *Service Life Prediction of Polymers and Plastics Exposed to Outdoor Weathering*; White, C. C.; White, K. M.; Pickett, J. E., Eds.; Plastics Design Library; William Andrew Publishing: Cambridge, MA, USA, **2018**. p. 95.
10. Pickett, J. E.; Gibson, D. A.; Gardner, M. M. *Polym. Degrad. Stab.* **2008**, 93, 1597.
11. Escobar, L. A.; Meeker, W. Q. *Stat. Sci.* **2006**, 21, 552.
12. Bauer, D. R. *Polym. Degrad. Stab.* **2000**, 69, 307.
13. ASTM International. ASTM WK55620: New Practice for Service Life Prediction of Polymeric Materials; ASTM International: West Conshohocken, PA.



14. ASTM International. ASTM WK57612: New Practice for Lifetime Prediction Using Equivalent Time in Weathering Test; ASTM International: West Conshohocken, PA.
15. Searle, N. D.; McGreer, M.; Zielnik, A. *Encyclopedia of Polymer Science and Technology*; John Wiley & Sons, Inc.: Hoboken, NJ, USA, **2002**.
16. Bruckman, L. S.; Wheeler, N. R.; Ma, J.; Wang, E.; Wang, C. K.; Chou, I.; Sun, J.; French, R. H. *IEEE Access*. **2013**, *1*, 384.
17. Pickett, J. E. In *Service Life Prediction of Exterior Plastics*; White, C. C.; Martin, J.; Chapin, J. T., Eds., Springer International Publishing: Switzerland, **2015**. p. 41.
18. Rubel, F.; Kotteck, M. *Meteorol. Z.* **2010**, *19*, 135.
19. Bryant, C.; Wheeler, N. R.; Rubel, F.; French, R. H. *kgc: Koeppen-Geiger Climatic Zones*; **2017**. Available at <https://CRAN.R-project.org/package=kgc>.
20. Pickett, J. E.; Gibson, D. A.; Rice, S. T.; Gardner, M. M. *Polym. Degrad. Stab.* **2008**, *93*, 684.
21. Parisi, A. V.; Turner, J. *Photochem. Photobiol. Sci.* **2006**, *5*, 331.
22. IEC TS82 62788-1-7. Measurement procedures for materials used in photovoltaic modules – Part 1-7: Test procedure for the optical durability of transparent polymeric PV packaging materials; International Electrotechnical Commission.
23. IEC TS82 62788-2-7. Measurement procedures for materials used in photovoltaic modules – Part 2-7: Environmental exposures-Accelerated weathering tests of polymeric materials; International Electrotechnical Commission.
24. Andrady, A. L. *Polymer Analysis Polymer Physics, Advances in Polymer Science*; Springer: Berlin, Heidelberg, **1997**. p. 47.
25. ASTM International. ASTM G154-16, Standard Practice for Operating Fluorescent Ultraviolet (UV) Lamp Apparatus for Exposure of Nonmetallic Materials; ASTM International: West Conshohocken, PA, **2016**.
26. ASTM International. ASTM D7869-17, Standard Practice for Xenon Arc Exposure Test with Enhanced Light and Water Exposure for Transportation Coatings; ASTM International: West Conshohocken, PA, **2017**.
27. Wypych, G.; Lee, F.; Pourdeyehimi, B. In *3rd International RILEM Symposium on Durability of Building and Construction Sealants*; Wolf, A. T., Ed., RILEM Publications: Cachan Cedex, France, **1999**. p. 173.
28. Edge, M.; Allen, N. S.; Wiles, R.; McDonald, W.; Mortlock, S. V. *Polymer*. **1995**, *36*, 227.
29. Edge, M.; Wiles, R.; Allen, N. S.; McDonald, W. A.; Mortlock, S. V. *Polym. Degrad. Stab.* **1996**, *53*, 141.
30. Allen, N. S.; Rivalle, G.; Edge, M.; Roberts, I.; Fagerburg, D. R. *Polym. Degrad. Stab.* **2000**, *67*, 325.
31. Gordon, D. A.; Zhan, Z.; Bruckman, L. S. *Polym. Degrad. Stab.* **2019**, in press.
32. Gok, A. Degradation Pathway Models of Poly(Ethylene-Terephthalate) under Accelerated Weathering Exposures; Case Western Reserve University: Cleveland, OH, United States, **2016**.
33. French, R. H.; Podgornik, R.; Peshek, T. J.; Bruckman, L. S.; Xu, Y.; Wheeler, N. R.; Gok, A.; Hu, Y.; Hossain, M. A.; Gordon, D. A.; Zhao, P.; Sun, J.; Zhang, G.-Q. *Curr. Opin. Solid State Mater. Sci.* **2015**, *19*, 212.
34. Gok, A.; Fagerholm, C. L.; Gordon, D. A.; Bruckman, L. S.; French, R. H. In *2015 I.E. 42nd Photovoltaic Specialist Conference (PVSC)*, **2015**.
35. Gok, A.; Ngendahimana, D. K.; Fagerholm, C. L.; French, R. H.; Sun, J.; Bruckman, L. S. *PLoS One*. **2017**, *12*, e0177614.
36. ASTM International. ASTM G173-03, Standard Tables for Reference Solar Spectral Irradiances: Director Normal and Hemispherical on 37° Tilted Surface; ASTM International: West Conshohocken, PA, **2012**.
37. Kockott, D. In *Durability Testing of Nonmetallic Materials*; Herling, R. J., Ed., ASTM International: West Conshohocken, PA, **1996**. p. 24.
38. ASTM International. ASTM E313, Practice for Calculating Yellowness and Whiteness Indices from Instrumentally Measured Color Coordinates; ASTM International: West Conshohocken, PA, **2015**.
39. ASTM International. ASTM D1003-13, Standard Test Method for Haze and Luminous Transmittance of Transparent Plastics; ASTM International: West Conshohocken, PA, **2013**.
40. White, K. M.; Burns, D. M.; Gregar, T. Q. In *Service Life Prediction of Exterior Plastics*; White, C. C.; Martin, J.; Chapin, J. T., Eds., Springer International Publishing Switzerland, **2015**. p. 21.
41. Grossman, D. The Myth of Reciprocity; Q-LAB: Westlake, OH, **2014**, Technical Article LW-6041. Available at <http://www.q-lab.com/documents/public/7a48025f-de8b-465d-8e4f-1ba1695367ee.pdf>.
42. National Solar Radiation Data Base. Typical Meteorological Year 3 (TMY3) Between 1991 and 2005. Available at: [https://rredc.nrel.gov/solar/old\\_data/nsrdb/1991-2005/tmy3/](https://rredc.nrel.gov/solar/old_data/nsrdb/1991-2005/tmy3/) (Accessed 18 October 2018).
43. Pickett, J. E.; White, K. M.; White, C. C. In *Service Life Prediction of Polymers and Plastics Exposed to Outdoor Weathering*; White, C. C.; White, K. M.; Pickett, J. E., Eds., *Plastics Design Library*; William Andrew Publishing: Cambridge, MA, USA, **2018**. p. 1.